Estimation of Aggregated Inertia Constant and Load Damping: A PMU-Based Analytical Approach

Hêmin Golpîra
Power Systems Modeling & Simulation Lab.,
Dept. of Electrical and Computer Engineering
University of Kurdistan
Kurdistan, Sanandaj, Iran
hemin.golpira@uok.ac.ir

Bruno Francois
Univ. Lille, Arts et Metiers Institute of Technology,
Centrale Lille, Junia, ULR 2697 - L2EP,
F-59000 Lille, France
bruno.francois@centralelille.fr

Bogdan Marinescu
Analysis and control of power grids, L2SN
Ecole Centrale Nantes
Nantes, France
bogdan.marinescu@ec-nantes.fr

Hassan Bevrani
Smart/Micro Grids Research Center
Dept. of Electrical and Computer Engineering
University of Kurdistan
Kurdistan, Sanandaj, Iran
bevrani@uok.ac.ir

***Abstract*—A precise, straightforward, and efficient data-driven methodology is introduced to estimate the most important aggregated generation-load parameters of the power system frequency response model i.e., the inertia constant and the load damping. The estimation method depends on defining specific base systems characterized by particular frequency features. A sensitivity analysis is carried out to determine the most suitable base system for each real-time application. The data collected from PMUs is then compared to the attributes of the base system to make accurate estimations of the parameters of interest. The effectiveness of the proposed methodologies is assessed using datasets that include both simulated data from the New York-New England benchmark and actual measurements collected from six historical power system disturbances within a national power grid.**

***Index Terms*—inertia constant, imbalance size, frequency dynamics, frequency modelling, load damping, RoCoF, system frequency response model.**

I. Introduction

The reliable and secure operation of modern power systems relies on the vital role played by frequency regulation mechanisms. The control loops engaged in frequency regulation are employed to ensure the frequency remains within a predetermined range during both transient and steady-state operational periods [1]. Hence, it is highly important to carry out thorough research into frequency response modeling. Accordingly, five different approaches have been proposed in the literature to tackle the modeling and prediction of frequency response [2]: 1) measurement-based modelling, as discussed in [3], [4] 2) time-domain simulation-based modeling, as discussed in [5], 3) linearized-based modeling, as explored in [6], 4) artificial intelligence-based modeling, as examined in [7], and 5) single-machine equivalent-based modeling, as elaborated in [8], [9].

Although local frequencies hold great significance in modern power systems, developing a system frequency response (SFR) model, belonging to the last category, is crucial for various reasons. Firstly, it provides a valuable tool for system operators (SOs) to determine and allocate the minimum necessary frequency response reserve [10]. Secondly, it enables the analysis of the impact of inverter-based resources on frequency regulation [11]. The key elements, however, within the SFR model that impact these objectives are linked to rotational inertia and load damping coefficients.

Generally, investigations into inertia and load damping estimation can be categorized into two approaches [12]: 1) model-based methods, and 2) measurement-based methods. The model-based inertia estimation approaches, relying on a dynamic model of synchronous generators (SGs), are essentially divided into single SG inertia estimation and regional system inertia estimation. Estimating the inertia of a single SG involves employing methods such as the extended Kalman filter [13], least-squares [14], optimization techniques [15], and various Kalman filter methods [16] when the generator is subjected to significant disturbances. The regional system inertia estimation, on the other hand, relies on developing a dynamic equivalent model for a group of coherent generators to estimate rotational inertia and load damping. This leads to a reduction in computational complexity when solving differential-algebraic equations with numerous SGs. Investigation into the development of a dynamic equivalent

model for SGs and loads, utilizing a genetic algorithm, is outlined in [17]. The division of dynamic equivalencing into two stages, covering mechanical and electrical components, is explored in [18]. In [19], the authors establish the dynamic equivalent for each area within a multi-area power system by defining the mathematical relationship between dynamic parameters and electromechanical oscillation parameters acquired from phasor measurement units (PMUs). It should be noted that the accuracy of the estimation in this category highly depends on the precision of the utilized model. Furthermore, relying on identifying coherent generators is another limitation of this category.

To overcome the challenges associated with the model-based approach, different inertia estimation strategies using PMU measurements have been proposed in recent years. This category is initially divided into two subcategories: 1) measurement-based inertia estimation using large disturbance data, and 2) measurement-based inertia estimation using ambient data. The former relies on the estimation of Rate of Change of Frequency (RoCoF) in the system to estimate the inertia constant. Estimation of RoCoF based on different approaches, including a 500 ms sliding window [20], variable-order polynomial fitting [21], and equivalent second-order homogeneous differential equation [22], are some approaches in this field. In contrast, techniques utilizing ambient data depend on data acquired from PMUs, representing the stochastic response time series of the system. In [23], the authors employ the Markov Gaussian approach for equivalent inertia estimation. The estimation of system inertia is expressed as a regression model in [4]. In most cases, research focused on deriving measurement-based parameter estimation primarily concentrates on estimating only rotational inertia, often overlooking the load damping parameter. However, for accurate results, these techniques require real-time data related to load levels, the composition of generation sources, the size of power imbalance, and the aggregated load model. Furthermore, a noteworthy challenge observed in previous research pertains to the reliance on the observability of the studied system.

In light of the aforementioned concerns, the current paper aims to propose a data-driven method to simultaneously estimate the inertia constant, the load damping factor, and the size of power imbalance. To address the difficulties related to system observability, the proposed approach involves estimating the parameters of interest through a comparison of frequency dynamics with a baseline frequency dynamic associated with a specific operating point of the system. Generally stated, the main contributions of this paper are twofold:

- Proposing an analytical approach to estimate inertia constant and load power imbalance for SFR model using PMU data.
- Proposing a mathematical approach to estimate load damping factor of the system.

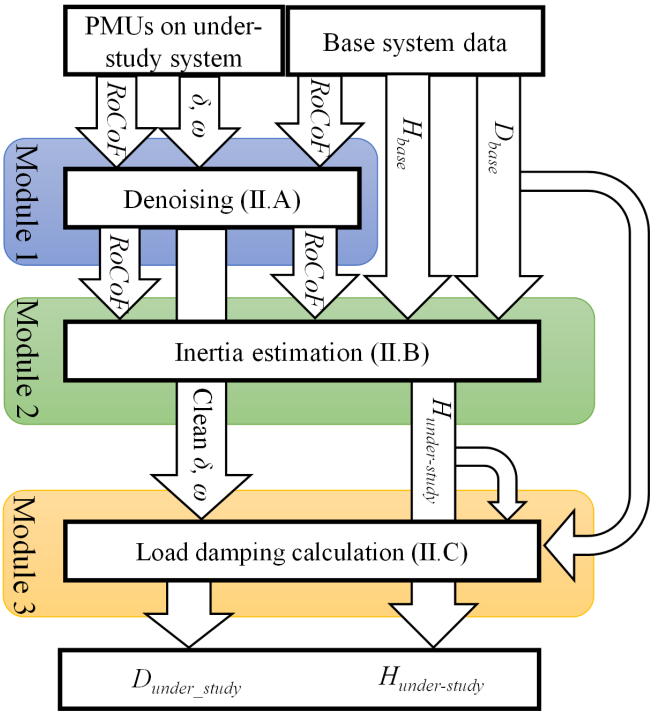

Fig. 1. A general description of the proposed estimation scheme.

II. Proposed Estimation Method

This section introduces a systematic method for estimating the key parameters in the SFR model. The suggested framework comprises three modules: 1) cleaning PMU signals, 2) determining the inertia constant and power imbalance magnitude, and 3) estimating the load damping factor. A diagram illustrating the proposed scheme, along with the input and output signals for each module, is presented in Fig. 1.

A. Data Denoising

Consider a vector, denoted as "**Freq**" with a length of L, representing noisy frequency measurements. Each element within "**Freq**" corresponds to the system's center of inertia (COI) based on measurements obtained from available PMUs. The primary aim is to derive a clean signal from the "**Freq**".

In a practical context, one can employ a moving-average window for the purpose of denoising the "**Freq**". Given a window of N samples, the implementation of the smoothing filter can be formally expressed using convolution notation as [24]:

$$\mathbf{F} = \frac{1}{N}(\mathbf{Freq} * \mathbf{I}) \tag{1}$$

where **F** and **I** denote the clean frequency signal and the unit vector of length N, respectively, and "*" is the convolution operator.

When examining a stability phenomenon under investigation, it is crucial to maintain the desired frequency components within the "**Freq**" data while effectively diminishing the influence of other frequency components. This can be accomplished by appropriately adjusting the parameter N in (1), as suggested by the same authors in [24], as

$$N \geq \frac{\sqrt{0.1962 + F_{CO}^2}}{F_{CO}} \tag{2}$$

where

$$F_{CO} = \frac{f_{co}}{f_s} \tag{3}$$

In (3), f_{co} and f_s represent the specific cut-off frequency and PMU sampling rate, respectively.

B. Inertia Constant Estimation

To calculate the aggregated inertia constant within the SFR model, the motion of the grid is expressed using the classical swing equation (4) [1].

$$2H \frac{\overbrace{d(\Delta\omega)}^{RoCoF}}{dt} = P^D \tag{4a}$$

where

$$\Delta\omega = \frac{\sum_{i=1}^{K} H_i \Delta\omega_i}{\sum_{i=1}^{K} H_i} \tag{4b}$$

In (4), H, H_i, ω and P^D represent the aggregated rotational inertia constant, inertia constant of generator i, average inertia-weighted angular speed, and size of power imbalance, respectively. Furthermore, K represents the number of PV buses equipped with PMUs.

Let's consider two power system models: 1) the base system, which characterized by specific parameters inertia constant H_{base}, power imbalance size P_{base}^D and droop R_{base}, and 2) the under-study system, which involves unknown inertia constant $H_{under-study}$. Assume that $H_{under-study}$ and $P_{under-study}^D$ can be represented incrementally as part of the evolving model (5).

$$\begin{cases} H_{under-study} = H_{base} + \Delta H \\ P_{under-study}^D = P_{base}^D + \Delta P^D \end{cases} \tag{5}$$

In this context, it is crucial to highlight that the base system and the under-study system are fundamentally identical, distinguished only by varying commitments of generating units and operational points. The characteristics of the base system, including the committed generating units, P_{base}^D, H_{base}, and RoCoF signal, can be easily obtained from historical data.

Now, the Taylor expansion of (4) is introduced to calculate $H_{under-study}$ and $P_{under-study}^D$ in (5), namely

$$\underbrace{RoCoF_{base} + \Delta RoCoF}_{RoCoF_{under-study}} = \frac{P_{base}^D}{2H_{base}} + \frac{1}{2H_{base}}\Delta P^D - \frac{2P_{base}^D}{4H_{base}^2}\Delta H \tag{6}$$

Drawing upon (6) and utilizing the definitions of parameters in (5), one has:

$$\Delta RoCoF = \frac{1}{2H_{base}}\left(P_{under-study}^D - P_{base}^D\right) - \frac{2P_{base}^D}{4H_{base}^2}\left(H_{under-study} - H_{base}\right) \tag{7}$$

Given that the left side of (7) is tailored to the measurements from PMUs, the current objective is to calculate two unspecified parameters $H_{under-study}$ and $P_{under-study}^D$. To complete the set of two equations with these two unknowns, one can express another relationship using (4).

In this context, it is important to emphasize that when addressing $RoCoF$ in (4) and (7), only the initial sample following the onset of the fault, referred to as $RoCoF_{\bullet}^{FS}$, is regarded as the influence of the governor, and load damping is minimal.

Further simplification can be attained by consolidating (4) and (7) into a more concise form of

$$\begin{bmatrix} \overbrace{RoCoF_{under-study}^{FS} - RoCoF_{base}^{FS}}^{\Delta RoCoF^{FS}} \\ 0 \end{bmatrix} = \begin{bmatrix} \frac{1}{2H_{base}} & \frac{P_{base}^D}{2H_{base}^2} \\ -1 & 2RoCoF_{under-study}^{FS} \end{bmatrix} \times \begin{bmatrix} P_{under-study}^D \\ H_{under-study} \end{bmatrix} - \begin{bmatrix} \frac{1}{2H_{base}} & \frac{P_{base}^D}{2H_{base}^2} \\ 0 & 0 \end{bmatrix} \begin{bmatrix} P_{base}^D \\ H_{base} \end{bmatrix} \tag{8}$$

By rearranging the terms in (8) and using the definition of P_{base}^D in (4) i.e., $P_{base}^D = 2H_{base} \times RoCoF_{base}^{FS}$, one has

$$\begin{bmatrix} P_{under-study}^D \\ H_{under-study} \end{bmatrix} = \frac{H_{base}}{RoCoF_{under-study}^{FS} + RoCoF_{base}^{FS}} \begin{bmatrix} 2RoCoF_{under-study}^{FS} & -\frac{P_{base}^D}{2H_{base}^2} \\ 1 & \frac{1}{2H_{base}} \end{bmatrix} \times \left\{ \begin{bmatrix} \Delta RoCoF^{FS} \\ 0 \end{bmatrix} + \begin{bmatrix} \frac{1}{2H_{base}} & \frac{P_{base}^D}{2H_{base}^2} \\ 0 & 0 \end{bmatrix} \begin{bmatrix} P_{base}^D \\ H_{base} \end{bmatrix} \right\} \tag{9}$$

Eq. (9) elucidates the inertia constant and disturbance magnitude within the under-study system by leveraging the established characteristics of the base system, along with the utilization of PMU data. The necessary prerequisite to obtain an accurate estimate of the variables using (9) is to have an equal number of PMUs for determining $RoCoF_{under-study}^{FS}$ and $RoCoF_{base}^{FS}$, i.e. K in (4b).

An important concern, however, lies in the selection of the base system to ensure accurate results in the under-study system. Since (9) relies on the Taylor expansion around the base system's operating point, opting for an unsuitable base case can lead to values that diverge significantly from the true values. To tackle this challenge, an analytical approach based on sensitivity analysis is recommended.

1) Sensitivity Analysis

Variations in operational conditions, such as different unit commitment configurations and changes in power imbalances, can potentially impact the effectiveness of the proposed method in accurately estimating under-study parameters. To assess this potential influence, a sensitivity analysis is conducted, focusing on the foundational characteristics of the base system. For this purpose, (7) is utilized to calculate the sensitivity of power mismatch size with respect to the base case operating condition, H_{base}, as follows:

$$P^D_{under-study} = \Big[RoCoF^{FS}_{under-study} - RoCoF^{FS}_{base} + \frac{P^D_{base}}{2H^2_{base}}\left(H_{under-study} - H_{base}\right)\Big] \times 2H_{base} + P^D_{base} \quad (10)$$

Rearranging of the terms in (10) gives

$$P^D_{under-study} = \left(RoCoF^{FS}_{under-study} - RoCoF^{FS}_{base}\right) \times 2H_{base} + \frac{P^D_{base} \times H_{under-study}}{H_{base}} \quad (11)$$

Now, let's express the sensitivity of power imbalance magnitude (11) with respect to the inertia constant using the Taylor expansion, as:

$$\Delta P^D_{under-study} = \frac{dP^D_{under-study}}{dH_{base}}\Delta H_{base} = 2\left(RoCoF^{FS}_{under-study} - RoCoF^{FS}_{base}\right)\Delta H_{base} - 2H_{base}\frac{dRoCoF_{base}}{dH_{base}}\Delta H_{base} - \frac{H_{under-study} \times P^D_{base}}{H^2_{base}}\Delta H_{base} \quad (12)$$

The second term on the right-hand side of (12) can be further simplified using the definition of RoCoF (4), leading to:

$$\Delta P^D_{under-study} = 2\left(RoCoF^{FS}_{under-study} - RoCoF^{FS}_{base}\right)\Delta H_{base} - \frac{P^D_{base}}{H_{base}}\Delta H_{base} - \frac{H_{under-study} \times P^D_{base}}{H^2_{base}}\Delta H_{base} \quad (13)$$

Rearranging the terms in (13) gives

$$\Delta P^D_{under-study} = 2\left(RoCoF^{FS}_{under-study} - RoCoF^{FS}_{base}\right)\Delta H_{base} + \frac{\left(H_{base} - H_{under-study}\right)}{H^2_{base}}\Delta H_{base} \quad (14)$$

Applying the identical steps outlined in (11) through (14) to ascertain the sensitivity of the under-study system to power imbalance size relative to the base system yields:

$$\Delta P^D_{under-study} = -2H_{base}\frac{dRoCoF_{base}}{dP^D_{base}}\Delta P^D_{base} + \frac{H_{under-study}}{H_{base}}\Delta P^D_{base} = \frac{H_{under-study} - H_{base}}{H_{base}} \times \Delta P^D_{base} \quad (15)$$

2) Technical Considerations

The second term on the right side of (14) becomes negligible and can be disregarded. Therefore, to minimize the impact of the base case inertia constant on the estimated power mismatch size, it is essential to maintain the *RoCoF* of both the base and under-study systems as close as possible. Moreover, the presence of the base system's inertia in the denominator of (15) indicates that opting for a base system with a higher inertia constant can significantly diminish the impact of the base system power imbalance size on the results. Consequently, it is deduced that to substantially reduce the sensitivity of (9) to the base case parameters, multiple base cases should be defined at the WAMS center. For each under-study system, immediately following a fault, the base case with a *RoCoF* closest to that of the under-study system should be chosen for the estimation process.

C. Load Damping Estimation

The second phase of the paper is dedicated to the estimation of load damping. To calculate the load damping factor, let's proceed by establishing the motion of the systems based on the synchronizing and damping torques. To this end, consider the original swing equation of (3) as

$$2H\frac{d^2\delta}{dt^2} = P_m - P_e \quad (16)$$

By re-writing the right-hand side of (16) based on the load-dependent and constant power (CP) loads, one obtains

$$2H\overbrace{\frac{d^2\delta}{dt^2}}^{\Delta\dot{\omega}} + D\overbrace{(\omega - 1)}^{\dot{\delta}} = P^{CP}_m - P^{CP}_e \quad (17)$$

For the purpose of estimating the damping factor, the expression on the right side of (17) can be rephrased using the representation of a single-machine infinite-bus equivalent model in the following manner:

$$P^{CP}_m - P^{CP}_e = \frac{V_g V_\infty cos\delta_0}{X_l + X'_d}\Delta\delta = K\Delta\delta \quad (18)$$

where V_g, V_∞, X_l, X'_d are the terminal voltage of the generator, terminal voltage of the equivalent grid, reactance of the transmission line, and transient impedance of the generator, respectively.

Considering the relationship $\Delta\dot{\delta} = \Delta\omega$ in addition to the definition provided in (18), (17) can be expressed in its final form as

$$\Delta\dot{\omega} = -\frac{K}{2H}\Delta\delta - \frac{D}{2H}\Delta\omega \quad (19)$$

If the system under investigation is fully observable, then, with the availability of data from PMUs for $\Delta\delta$, $\Delta\omega$, and *RoCoF*, it becomes possible to construct a curve in the following format:

$$\Delta\dot{\omega} = A\Delta\delta + B\Delta\omega \quad (20)$$

It is crucial to emphasize that the values of constants A and B in (20) are established through the curve fitting procedure. Then, with H obtained from (9), one could express D as:

$$-\frac{D}{2H} = B \rightarrow D = -2H \times B \quad (21)$$

However, to compute damping in systems with a limited number of PMUs and address observability concerns, let's return to the base system once again. Accordingly, one can write (19) for the base system as:

$$\Delta\dot{\omega}_{base} = -\frac{K_{base}}{2H_{base}}\Delta\delta_{base} - \frac{D_{base}}{2H_{base}}\Delta\omega_{base} \quad (22)$$

Furthermore, one has (22) for the under-study system as

$$\Delta\dot{\omega}_{under-study} = -\frac{K_{under-study}}{2H_{under-study}}\Delta\delta_{under-study} - \frac{D_{under-study}}{2H_{under-study}}\Delta\omega_{under-study} \quad (23)$$

The contrast between the two second terms on the right-hand side of (22) and (23) can be substantiated by employing a Taylor expansion of the form

$$\left(\frac{D}{2H}\right)_{under-study} - \left(\frac{D}{2H}\right)_{base} = \frac{\Delta\omega_{base}}{2H_{base}}\Delta D - \frac{2D_{base}\Delta\omega_{base}}{4H^2{}_{base}}\Delta H \quad (24)$$

Considering that the left side of (24) is obtained from the fitted curves, ΔD represents the only unspecified parameter. Once ΔD is calculated, one can express $D_{under-study}$ as:

$$D_{under-study} = D_{base} + \Delta D \quad (25)$$

III. Application Results

Exploratory investigations are carried out to evaluate the efficacy of the suggested formulations, employing both simulated and actual measured data.

The initial study demonstrates the application of the methods to noise-free observational data. Data derived from transient stability simulations of the 68-bus New York-New England (NYNE) test system, using MATLAB 2018b, which includes the power system toolbox (PST) [25], were used to assess the accuracy of the developed procedures. Fig. 2 presents a single-line diagram of the NYNE test system, displaying generator buses with PMUs and the locations of breakers where contingencies are applied. Detailed models of generating units and their controllers were incorporated into the simulations. Specifically, generators G_1 to G_{12} were equipped with fourth-order type II power system stabilizers, tuned to offer adequate damping [26].

Measured data from eight disturbance events, recorded by PMUs using a sampling rate of 60 Hz, in the NYNE test system are used to assess the efficiency of the proposed formulations. It is assumed that scenarios related to the tripping of generator number 12 and shedding of load at bus 52 are considered as the base systems. Results reported in Table I show high efficiency of the proposed method to estimate the parameters of interest in the system.

For instance, consider the shedding of load at bus 49. Substituting the measured quantities into (9) and taking into account the base system of load shedding at bus 52 yields

$$\begin{bmatrix} P^D_{under-study} \\ H_{under-study} \end{bmatrix} = \frac{5.50}{0.0053 + 0.0051} \begin{bmatrix} 2 \times 0.0053 & -\frac{0.0545}{2(5.50)^2} \\ 1 & \frac{1}{2(5.50)} \end{bmatrix} \times \left\{ \begin{bmatrix} 0.0053 - 0.0051 \\ 0 \end{bmatrix} + \begin{bmatrix} \frac{1}{2(5.50)} & \frac{0.0545}{2(5.50)^2} \\ 0 & 0 \end{bmatrix} \begin{bmatrix} 0.0545 \\ 5.50 \end{bmatrix} \right\} = \begin{bmatrix} 0.0567 \\ 5.3462 \end{bmatrix} \quad (26)$$

In another attempt, Fig. 3 illustrates the trajectories of synchronizing and damping torques, with Fig. 3(a) related to the base system represented using (22), as

$$\Delta\dot{\omega}_{base} = 0.0034\Delta\delta_{base} + 1.073\Delta\omega_{base} \quad (27)$$

Moreover, one can express the under-study system as:

$$\Delta\dot{\omega}_{under-study} = 0.0127\Delta\delta_{under-study} + 1.287\Delta\omega_{under-study} \quad (28)$$

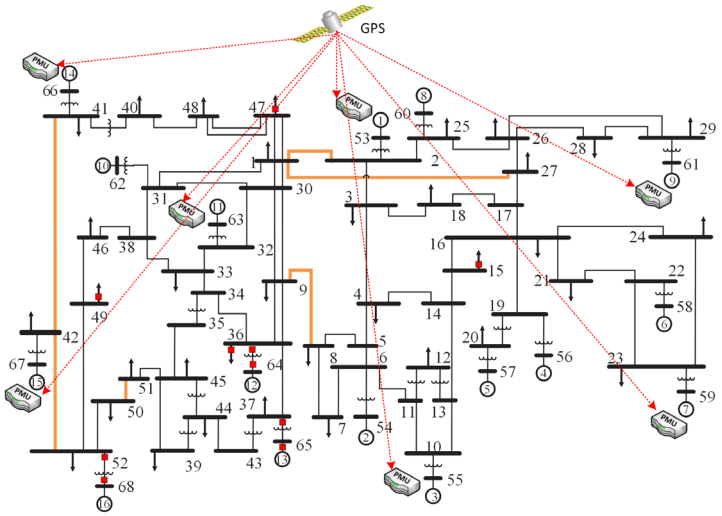

Fig. 2. Single line diagram of the 68-bus system showing PMUs locations. Red points indicate locations of breakers where contingencies are applied.

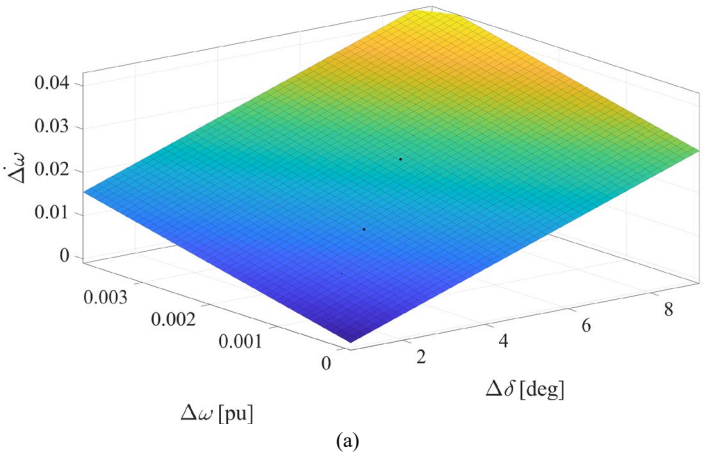

(a)

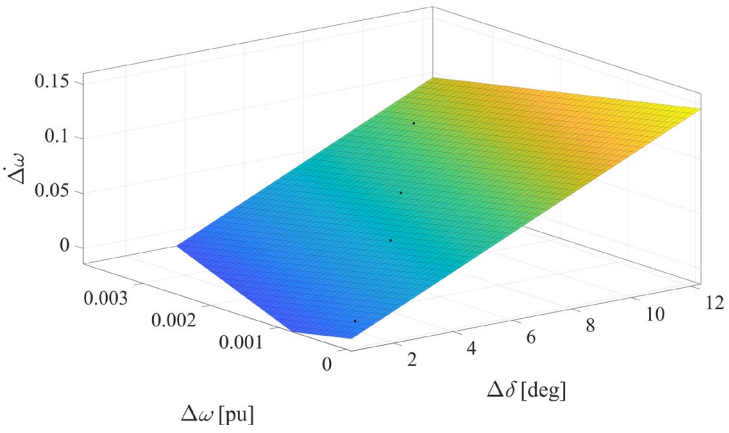

(b)

Fig. 3. Trajectory of synchronizing and damping torques in response to shedding of load at bus 37; a) base system, b) under-study system.

The coefficient of determination, R^2, for (27) and (28), derived from 30 samples, is 0.9982 and 0.09892, respectively, indicating a highly accurate fitness.

TABLE I
ESTIMATION OF FREQUENCY RESPONSE MODEL PARAMETERS FOR VARIOUS LOAD AND GENERATION TRIPPING SCENARIOS

Scenario	H_{est}	H_{real}	$P^{D}_{L,est}$	$P^{D}_{L,real}$	D_{est}	D_{real}
L_{26}	5.0142	5.02	0.0521	0.05	1.88	1.8
L_{3}	6.2267	6.30	0.077	0.076	1.12	1.1
L_{46}	4.9718	5.10	0.316	0.309	2.16	2.1
L_{49}	5.3462	5.30	0.0567	0.060	4.401	4.40
L_{52}	**-**	**5.50**	**-**	**0.0545**	**-**	**3**
G_{12}	**-**	**5.15**	**-**	**0.065**	**-**	**1.6**
G_{8}	4.0461	4.10	0.0645	0.0635	2.93	3
G_{14}	3.7513	3.85	0.0931	0.0950	3.78	3.8

TABLE II
ESTIMATION OF THE POWER IMBALANCE AND THE INERTIA

	D_{est}	D_{real}	Error	H_{real}	H_{est}	Error
Event 1	3.16	3.2	1.25%	4.5047	4.4873	0.39%
Event 2	4.87	-	-	6.4767	-	-
Event 3	4.23	4.25	0.4%	2.9653	3.0041	1.31%
Event 4	5.12	-	-	2.5924	-	-
Event 5	4.92	5	1.6%	2.6355	2.6566	0.10%
Event 6	3.54	-	-	9.2289	-	-
Event 7	3.49	3.50	0.28%	5.8455	5.8900	0.70%
Event 8	4.22	4.16	1.44%	8.0710	8.2103	1.72%
Event 9	2.50	2.48	0.81%	7.3116	7.3009	~0.00%

To calculate the damping factor for the under-study system, let us substitute the quantities into (24) as follows:

$$1.287 - 1.073 = \frac{2 \times \pi(50 - 49.87)}{5.50}\Delta D - \frac{2 \times 3 \times 2 \times \pi(-50 + 49.87)}{4(5.50)^2}(5.50 - 5.3462) \rightarrow \Delta D = 1.401 \quad (29)$$

Then, one can calculate the damping factor as

$$D_{under-study} = \Delta D + D_{base} \rightarrow D_{under-study} = 1.401 + 3 \rightarrow D_{under-study} = 4.401 \quad (30)$$

The second study examines the application of the methods to actual data. Measured data recorded by PMUs using a 25 Hz sampling rate in the national power grid are used to assess the efficacy of the proposed formulations. The grid has 16 regional electric companies with a 50 Hz nominal frequency and 76428 MW capacity [27].

The primary objective is to extract the clean signal from the recorded signal. This clean signal is defined as the inertia-weighted average of data collected from PV buses. Considering a theoretical cut-off frequency of 1.5 Hz for slow power and frequency variations [24], one can determine the minimum required number of samples to be averaged using (2), namely

$$N = \frac{\sqrt{0.1962 + (\frac{1.5}{25})^2}}{(\frac{1.5}{25})} \cong 8 \quad (31)$$

Comparison of the original and the noise-free signals, obtained by setting N equal to 8 in (1) in Fig. 4, shows the ability of the smoothing filter (1) to denoise the PMU data.

After obtaining the clean signal, the efficiency of the developed procedure in estimating the inertia constant and load damping factor is tested through nine distinct contingency scenarios. These scenarios involve significant generation outages and are used to assess the accuracy of the proposed procedures in real-world large-scale applications. For the estimation procedures, three scenarios associated with events number 2, 4 and 6 are regarded as the base systems.

Table II presents the estimated parameters and the disparities between the observed and estimated values. The findings illustrate the strong effectiveness of the suggested approach in estimating the SFR model of the system in real time application. For example, consider Event 3 in Table II, where employing the identical process as detailed in (26) and designating Event 4 as the reference system results in an inertia constant of 2.9653. The RoCoF difference between Events 3 and 4 is approximately 0.0018 Hz, which is lower than the disparities observed with other base systems, highlighting the improved accuracy when utilizing Event 4 as the base case.

In this context, it is important to highlight that, given the variation in RoCoFs across the scenarios under investigation, three base systems with a 0.002 Hz range have been chosen. However, opting for more base systems with narrower RoCoF spans can lead to enhanced accuracy; for example, consider Event 8 in Table II. Errors for D and H, totaling 1.44% and 1.72%, respectively, are observed with the current three base systems. These discrepancies can be reduced to as little as 0.14% and 0.05%, respectively, by increasing the number of base systems to six, each with a 0.001 Hz span.

IV. DISCUSSION

The implementation of the proposed estimation method requires consideration of a number of issues:

1- Since (9) utilizes the first sample of RoCoF after the inception of the fault to estimate the parameters of interest, the estimation procedure in this paper is only possible after a disturbance. To achieve this objective, it is assumed that the initiation of a fault may activate the estimation procedure. The frequency event is identified when the clean frequency signal exhibits an increasing/decreasing trend over five consecutive observations [28].

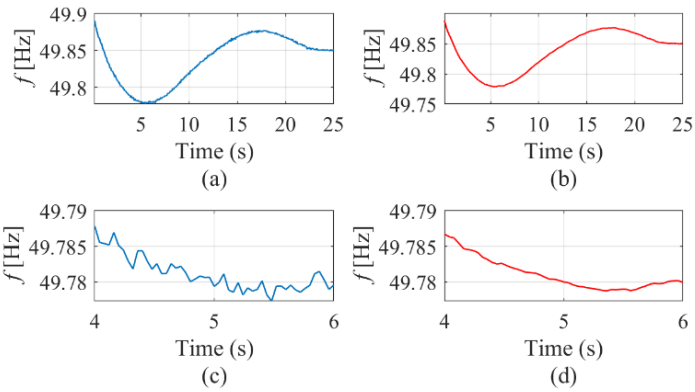

Fig. 4. Denoising of PMU signal by a window of length 8 samples; a) noisy signal, b) clean signal, c) zoomed noisy signal in the range of 4 sec to 6 sec, d) zoomed clean signal in the range of 4 sec to 6 sec.

2- Regional inertia in the system can be estimated based on the center-of-gravity (COG) concept in [3], where the ratio of local frequencies to the frequency of the SFR model over time is expressed in terms of the ratio of regional inertia to the inertia calculated in (9). More precisely, regional inertia can be computed by acquiring local frequencies from PMUs and deducing the global frequency associated with SFR using the parameters of interest in this paper.

V. CONCLUSION

This research contributes to the development of an effective method for estimating the primary parameters of the aggregated SFR model of a power grid based on PMU data, offering valuable insights for power system control. The method relies on defining frequency dynamics associated with certain historical events within the system to estimate inertia constant and load damping in real-time applications. The findings from applying the method to both real and simulated data illustrate that the establishment of a set of historical frequency dynamics for utilization in various real-time scenarios significantly enhances result accuracy. The key indicator for selecting the most appropriate base system from the predefined set is determined to be the first sample of *RoCoF* after the inception of a fault. Reliance on defining base systems means that the requirement for system observability, which necessitates a substantial number of PMUs, is no longer considered a prerequisite for implementation in practical systems. The suggested approach is well-suited and holds promise for real-time applications due to its advantageous features of low computational requirements and high accuracy.

References

[1] H. Golpîra, A. Román-Messina, and H. Bevrani, *Renewable Integrated Power System Stability and Control*. John Wiley & Sons, 2021.

[2] H. Huang *et al.*, "Generic system frequency response model for power grids with different generations," *IEEE Access,* vol. 8, pp. 14314-14321, 2020.

[3] H. Golpîra and A. R. Messina, "A center-of-gravity-based approach to estimate slow power and frequency variations," *IEEE Transactions on Power Systems,* vol. 33, no. 1, pp. 1026-1035, 2017.

[4] J. Schiffer, P. Aristidou, and R. Ortega, "Online estimation of power system inertia using dynamic regressor extension and mixing," *IEEE Transactions on Power Systems,* vol. 34, no. 6, pp. 4993-5001, 2019.

[5] P. Ju, Y. Zheng, Y. Jin, C. Qin, Y. Jiang, and L. Cao, "Analytic assessment of the power system frequency security," *IET Generation, Transmission & Distribution,* vol. 15, no. 15, pp. 2215-2225, 2021.

[6] J. Dong, X. Ma, S. M. Djouadi, H. Li, and Y. Liu, "Frequency prediction of power systems in FNET based on state-space approach and uncertain basis functions," *IEEE Transactions on Power Systems,* vol. 29, no. 6, pp. 2602-2612, 2014.

[7] Q. Wang, C. Zhang, Y. Lü, Z. Yu, and Y. Tang, "Data inheritance–based updating method and its application in transient frequency prediction for a power system," *International Transactions on Electrical Energy Systems,* vol. 29, no. 6, p. e12022, 2019.

[8] P. M. Anderson and M. Mirheydar, "A low-order system frequency response model," *IEEE transactions on power systems,* vol. 5, no. 3, pp. 720-729, 1990.

[9] J. Shen, W. Li, L. Liu, C. Jin, K. Wen, and X. Wang, "Frequency response model and its closed-form solution of two-machine equivalent power system," *IEEE Transactions on Power Systems,* vol. 36, no. 3, pp. 2162-2173, 2020.

[10] H. Golpîra and B. Marinescu, "Enhanced Frequency Regulation Scheme: An Online Paradigm for Dynamic Virtual Power Plant Integration " *IEEE Transactions on Power Systems,* 2024, doi: 10.1109/TPWRS.2024.3368796.

[11] H. Bevrani, H. Golpîra, A. R. Messina, N. Hatziargyriou, F. Milano, and T. Ise, "Power system frequency control: An updated review of current solutions and new challenges," *Electric Power Systems Research,* vol. 194, p. 107114, 2021.

[12] B. Tan, J. Zhao, M. Netto, V. Krishnan, V. Terzija, and Y. Zhang, "Power system inertia estimation: Review of methods and the impacts of converter-interfaced generations," *International Journal of Electrical Power & Energy Systems,* vol. 134, p. 107362, 2022.

[13] M. Namba, T. Nishiwaki, S. Yokokawa, and K. Ohtsuka, "Idenntification of parameters for power system stability analysis using Kalman filter," *IEEE Transactions on Power Apparatus and Systems,* no. 7, pp. 3304-3311, 1981.

[14] Y. Wehbe, L. Fan, and Z. Miao, "Least squares based estimation of synchronous generator states and parameters with phasor measurement units," in *2012 North American Power Symposium (NAPS)*, 2012: IEEE, pp. 1-6.

[15] E. P. T. Cari and L. F. C. Alberto, "Parameter estimation of synchronous generators from different types of disturbances," in *2011 IEEE power and energy society general meeting*, 2011: IEEE, pp. 1-7.

[16] A. Rouhani and A. Abur, "Constrained iterated unscented Kalman filter for dynamic state and parameter estimation," *IEEE Transactions on Power Systems,* vol. 33, no. 3, pp. 2404-2414, 2017.

[17] E. L. Geraldi Jr, T. C. Fernandes, A. B. Piardi, A. P. Grilo, and R. A. Ramos, "Parameter estimation of a synchronous generator model under unbalanced operating conditions," *Electric Power Systems Research,* vol. 187, p. 106487, 2020.

[18] S. Nabavi and A. Chakrabortty, "Structured identification of reduced-order models of power systems in a differential-algebraic form," *IEEE Transactions on power systems,* vol. 32, no. 1, pp. 198-207, 2016.

[19] D. Yang *et al.*, "Data-driven estimation of inertia for multiarea interconnected power systems using dynamic mode decomposition," *IEEE Transactions on Industrial Informatics,* vol. 17, no. 4, pp. 2686-2695, 2020.

[20] P. Ashton, G. Taylor, A. Carter, M. Bradley, and W. Hung, "Application of phasor measurement units to estimate power system inertial frequency response," in *2013 IEEE Power & Energy Society General Meeting*, 2013: IEEE, pp. 1-5.

[21] C. Phurailatpam, Z. H. Rather, B. Bahrani, and S. Doolla, "Measurement-based estimation of inertia in AC microgrids," *IEEE Transactions on Sustainable Energy,* vol. 11, no. 3, pp. 1975-1984, 2019.

[22] R. K. Panda, A. Mohapatra, and S. C. Srivastava, "Online estimation of system inertia in a power network utilizing synchrophasor measurements," *IEEE Transactions on Power Systems,* vol. 35, no. 4, pp. 3122-3132, 2019.

[23] X. Cao, B. Stephen, I. F. Abdulhadi, C. D. Booth, and G. M. Burt, "Switching Markov Gaussian models for dynamic power system inertia estimation," *IEEE Transactions on Power Systems,* vol. 31, no. 5, pp. 3394-3403, 2015.

[24] H. Golpîra, H. Bevrani, A. R. Messina, and B. Francois, "A data-driven under frequency load shedding scheme in power systems," *IEEE Transactions on Power Systems,* vol. 38, no. 2, pp. 1138-1150, 2023.

[25] P. W. Sauer, M. Pai, and J. H. Chow, "Power system toolbox," 2017.

[26] G. Rogers, *Power system oscillations*. Springer Science & Business Media, 2012.

[27] A. A. Majd, E. Farjah, and M. Rastegar, "Composite generation and transmission expansion planning toward high renewable energy penetration in Iran power grid," *IET Renewable Power Generation,* vol. 14, no. 9, pp. 1520-1528, 2020.

[28] "PMU placement and installation," in "Guideline, NERC Reliability," NERC, Atlanta, GA, USA, 2016. [Online]. Available: https://www.nerc.com/comm/RSTC_Reliability_Guidelines/Reliability%20Guideline%20-%20PMU%20Placement.pdf